THE UNIVERSITY of EDINBURGH

Edinburgh Research Explorer

Multi-objective optimization for an integrated renewable, power-to-gas and solid oxide fuel cell/gas turbine hybrid system in microgrid

Citation for published version:
Ding, X, Sun, W, Harrison, G, Lv, X & Weng, Y 2020, 'Multi-objective optimization for an integrated renewable, power-to-gas and solid oxide fuel cell/gas turbine hybrid system in microgrid', *Energy*, vol. 213, 118804. https://doi.org/10.1016/j.energy.2020.118804

Digital Object Identifier (DOI):
10.1016/j.energy.2020.118804

Link:
Link to publication record in Edinburgh Research Explorer

Document Version:
Peer reviewed version

Published In:
Energy

General rights
Copyright for the publications made accessible via the Edinburgh Research Explorer is retained by the author(s) and / or other copyright owners and it is a condition of accessing these publications that users recognise and abide by the legal requirements associated with these rights.

Take down policy
The University of Edinburgh has made every reasonable effort to ensure that Edinburgh Research Explorer content complies with UK legislation. If you believe that the public display of this file breaches copyright please contact openaccess@ed.ac.uk providing details, and we will remove access to the work immediately and investigate your claim.

Download date: 04. May. 2023

Multi-objective optimization for an integrated renewable, power-to-gas and solid oxide fuel cell/gas turbine hybrid system in microgrid

Xiaoyi Ding[a,b], Wei Sun[b,*], Gareth P. Harrison[b], Xiaojing Lv[c,*], Yiwu Weng[a]

a. School of Mechanical Engineering, Key Laboratory for Power Machinery and Engineering of Ministry of Education, Shanghai Jiao Tong University, Shanghai, 200240, China

b. School of Engineering, University of Edinburgh, Mayfield Road, Edinburgh EH9 3DW, UK

c. Research Center for Low Carbon Combustion and Engine System, China-UK Low Carbon College, Shanghai Jiao Tong University, Shanghai, 201306, China

Abstract:

Power-to-gas (P2G) using excess renewable sources is an effective method to reduce renewable curtailment issues in microgrid system. The produced hydrogen is versatile green fuel for different energy sectors, such as electricity, heat and mobility. In recent researches, fuel cell-based system is considered as a promising technology to consume hydrogen (H_2) generated from P2G due to high efficiency and cleanness. However, its economic and thermodynamic adaptability when coupled with intermittent renewable sources remains an open question to be addressed carefully. One of the major challenges in optimizing such system is to simultaneously capture the intraday and seasonal variation of renewable sources & load, as well as the internal thermodynamic process of critical components in appropriate modeling detail. This paper presents a multi-energy system for microgrid in which a wind-powered P2G is coupled with a detailed thermoeconomic model of solid oxide fuel cell/gas turbine (SOFC/GT) hybrid system. A two-level multi-objective optimization of planning and operation together is proposed. For system planning, the optimal balance between the least wind curtailment rate and total life cycle cost (LCC) is determined. To facilitate the coordinate operation of system components, a power management strategy is proposed in response to fluctuations of wind power and

* Corresponding authors (w.sun@ed.ac.uk, lvxiaojing@sjtu.edu.cn).

electricity load with considerations of multiple thermodynamic safety criteria. Results show that in the selected case, the multi-energy system operates with low wind curtailment rate of 0.63% and high renewable penetration level of 90.1%. The optimized LCC of multi-energy system is £2,468,093 with wind power accounting for 68.35% of total capital investment. With the power management strategy applied, the SOFC/GT could operate under the maximum electrical efficiency of 67.1% with safety constraints satisfied, making up only half investment cost of P2G. To capture seasonal variations, both winter and summer scenarios are detailly analyzed, sensitivity analysis is also carried out to evaluate the interaction between capacities of MES components.

Keywords: Solid oxide fuel cell; gas turbine; power-to-gas; renewable energy; multi-energy system; multi-objective optimization.

1. Introduction

Renewable energy sources (wind, solar, hydro, biomass, etc.) are becoming increasingly popular around the world due to environmental issues such as global warming and shortage of fossil fuel. For example. the UK government has committed to reducing all greenhouse gas emissions to net-zero by 2050 [1]. These ambitious targets make the high penetration of renewable energy into energy supply mix an inevitable choice. In recent years, distributed energy systems based on wind and solar power, often formed as microgrids, have been gaining more and more attention.

In a microgrid system, limited by the power scale and additional investment of cross-region transportation, improving the self-consumption of renewable energy becomes a major issue [2]. Given that the fluctuation of renewable sources, high renewable energy penetration could help self-sufficiency but also bring challenges to balance supply and demand. One promising technology to increase the flexibility of renewable energy system in microgrid is Power-to-Gas (P2G). P2G system produces hydrogen (H_2) through water electrolyser when there is an excess supply of renewable electricity, and stores H_2 for later use when the electricity supply becomes short. With its high heat value and zero-pollution, using H_2 directly could greatly improve the local utilization of renewable sources in microgrid, yet requiring efficient H_2 consuming technology to form an integrated multi-energy system (MES). In such a case, solid oxide fuel cell (SOFC), without the limitation of Carnot cycle [3][4], could transfer chemical energy of H_2 directly into electricity through clean and efficient thermoelectric reaction. SOFC has high efficiency, low environmental emission, good fuel adaptability, as well as flexible combinability with other power systems [5]. Combined with a micro gas turbine (GT), the SOFC/GT hybrid system is a reliable electricity generation method to be coupled with renewable and P2G.

In the literature, different aspects of renewable energy systems based on P2G and fuel cells have been investigated. Al-musleh et al. [6] presented an integrated system of P2G with an electrolyser, methanation and

co-generation using a SOFC, and results showed that round trip efficiency could reach 55%. Hosseini et al. [7] studied a hybrid PV/FC system and results showed that the maximum total energy and exergy efficiency reached 55.7% and 49%, respectively. Wang et al. [8] studied a hybrid wind/PV/FC energy system for off-grid application. An overall strategy was designed to manage power flows among different components. Silva et al. [9] studied the optimal design of a PV/FC/electrolyser/battery system. The optimization of hybrid system by HOMER software is performed to reduce the cost. Yang et al. [10] proposed a sizing methodology in a PV/wind hybrid system based on genetic algorithm (GA). Ghaffari et al. [11] proposed design optimization of a hybrid system consisting of PV/electrolyser/diesel. Renewable energy portion (REP) was used as a constraint to evaluate renewable energy penetration. Suciu et al. [12] proposed a hybrid P2G/SOFC/GT in a CO_2 network for urban heating. An economic analysis was carried out and the influence of waste recovery equipment on system sizing was discussed. Gorre et al. [13] carried out a cost benefit optimization on a P2G and methanation system. Power sources like wind, solar and electricity were included in the configuration and compared respectively. Colombo et. al. [14] analyzed the installed microgrid system in the University of California, Irvine campus. The energy system consisted of PV, gas turbine, P2G and a 300kW solid oxide electrolysis (SOE) facility. Results showed that 58% of the renewable production would be temporally in excess of demand and would have to be stored or curtailed. Vahid et. al. [15] researched the energy management issue in the multi-energy system with PV and wind. Three strategies which include storing the surplus power by electrical storage, converting the extra power to the hydrogen by P2G as energy carrier and transferring the surplus power to the main grid were discussed and compared. The optimization of P2G capacity for access renewable had been achieved for cost and pollution functions. Choudhary et. al. [16][17] presented a thermodynamic study on optimizing a hybrid system of SOFC and recuperative gas turbine with air-film cooling of blades, performance maps of fuel cell and system were carried out specifically, and the results indicated that optimization for complex system involving energy & mass flows is necessary and beneficial for performances

[18][19]. Cao et. al. [20] presented a study on solar/P2G/SOFC/SOEC system, exergy and economic studies were carried out. Different optimization algorithms were compared based on optimization results. Gholamian et. al. [21] studied a multi-energy system of electrolysis/SOFC/GT using biomass as fuel. Output power from gas turbine is used to support electrolysis (PEME) to generate hydrogen. Optimization on system design for maximum exergy efficiency was carried out. Zhang et. al. [22] presented an electricity-gas energy system of P2G/SOEC/GT and gas networks, the impacts of injecting hydrogen to the natural gas pipeline were quantified. However, the coordination operation of each components with respect of thermodynamic criteria was not included.

From the literature review, only a few researches focused on the multi-energy system consisting of renewable sources, P2G and SOFC/GT. Although this concept has been introduced in some studies, these works mainly focus on either schematic planning [12][21] or operation [14][20][22] and lack enough depth on thermal adaptability and safety function. However, when the thermodynamic complexity of MES system increases with its structure, the capacity planning and operational function of system become firmly bonded in thermal, economical and manufactural perspectives. Especially for the wind/P2G/SOFC/GT system in the paper, its thermal complexity and non-linear feature could bring a series of challenges: 1) In our previous works [23][24], it is found that the operation window of SOFC/GT is a result of complicated trade-offs by multiple safety risks, including SOFC three-phase boundary overheat, heat stress caused by SOFC temperature gradient, GT power mismatch, compressor surge and tolerance temperature of turbine blade material, etc. 2) The safety margins of fuel cell, compressor and turbine are non-linear and thermo-coupled parameters related with capacity scale, and dangerous operation might result in power mismatch, irreversible damage and breakdown of performances [23], which must be avoided during the dynamic operation of the MES system for all the time. 3) Current researches mainly put emphasis on the basic mass and power constraints [25], yet lacking enough detail on the thermodynamic constraints of multiple components.

Furthermore, the intermittency and randomness of renewable energy sources (wind, solar, etc.) bring additional challenges for system planning and operation. Note that in the MES system, subcomponents are bonded with high degree of energy & mass coupling flows, this feature could leave significant impact on the interactive pattern between components. On the one hand, the expected power output from the SOFC/GT is driven by the load gap between wind/solar availability and local demand. However, due to the intermittent nature of renewable sources, the amount of this gap is random and could possibly fall out of SOFC/GT safety range. On the other hand, the available amount of H_2 in the storage is determined by the P2G process and could not always meet the demanded H_2 flowing rate of SOFC/GT, which would result in dangerous operation. Therefore, SOFC/GT in the multi-energy system could frequently face mismatch and unbalance in both electricity demand and fuel supply sides. Considering that SOFC/GT consists of several subsystems, multiple input parameters (fuel, air, etc.) [23][21], and narrow operating window as mentioned above, these factors could result in the multi-energy system facing serious risks of safe operation, which indicates that handling the coordinates of all components is essential in evaluating and optimizing such a system.

From what is discussed above, the adaptability of SOFC/GT with a renewable-powered P2G plant in the proposed system needs to be evaluated carefully. To realize high reliability and renewable consumption, optimization of such a system should be conducted to solve simultaneously the MES planning and operation of complex flowsheets, which has not been deeply carried out before. To be specific, the authors believe that the following aspects should be taken into consideration: 1) Thermodynamic safety criteria of each critical components. 2) Fluctuations of renewable sources and power load in a long-term operation. 3) Coordination principle of multiple components bonded with energy & mass flows. 4) Algorithm capable of handling different time scales for optimization in both planning and operation levels.

To address the research questions outlined above, based on our previous work [23][26], this paper presents a multi-objective optimization on the MES system of wind power, P2G, H_2 storage and SOFC/GT

for microgrid. Detailed thermodynamic model of SOFC/GT is established on MATLAB/Simulink platform and coupled with P2G system. A two-level modeling approach for optimization is applied during this research. At the operational level, to address the coordinate operation of wind power, P2G and SOFC/GT, a power management strategy is proposed in response to wind & demand fluctuations. Amount of wind used for local demand and electrolysis, H_2 charged/discharged in storage and generation level of SOFC and gas turbine are collected at each timestep. In the planning level, the optimal sizing of the integrated system is determined by considering both life-cycle cost (LCC) and wind curtailment rate as the objective functions. The whole model is optimized by multi-objective method using genetic algorithm. Finally, case study and sensitivity analysis are carried out based on the results of optimization from Pareto Front.

To the best of the authors' knowledge, multi-objective optimization on the integrated wind-powered P2G plant with a full-detailed model of SOFC/GT has not been fully studied before. The methodology in this work could provide theoretical guidance for component matching, optimization design and parameter selection. The proposed modeling and evaluation framework could improve the understanding of the value of SOFC/GT in renewable P2G-based system, and would also facilitate its implementation in helping the low carbon energy transition. Based on the literature listed above, the comparison of related MES studies with the proposed one are given in Table 1. As a result, the main contribution of the present work could be summarized as follows:

• Designing an integrated wind-powered P2G/SOFC/GT system, with a detailed thermodynamic model to capture internal safety criteria of critical components.

• Optimizing the system in two-level multi-objective method including different time scales to achieve both low wind curtailment rate and life-cycle cost.

• Taking into account the regular unbalance problem between intermittency of wind sources and safe operating window of SOFC/GT, a novel power management strategy is proposed for coordination.

• Examining the feasibility of the system based on case study under high renewable penetration.

Table 1 Comparison of proposed and previous studies

References	[8]	[11]	[12]	[13]	[14]	[15]	[20]	[21]	[22]	The proposed study
Wind/P2G/SOFC/GT configuration			√		√		√		√	√
Optimizations on planning or operation		√		√		√	√	√		√
Thermodynamic modeling and safety criteria	√						√	√		√
Subsystem coordination strategy	√	√			√	√			√	√
Wind uncertainties	√	√	√	√	√	√		√	√	√

2. System Structure and Description

2.1. System Structure

The configuration layout of multi-energy system with grid connection is shown in Figure 1, and it includes wind turbine, electrolyser, H_2 storage and SOFC/GT. Output from wind turbine is used to support local demand. Given the intermittency of renewables, in events when the wind power exceeds local demand, the excess ouput will be used by electrolysers to converts water into H_2, which is then kept in storage tank for later use. When the wind power is not sufficient to meet local demand, SOFC/GT will operate as a back-up power source to fill the gap. H_2 and air are preheated by the exhaust gas in heat exchanger 1 and 2 before flowing into SOFC. Then the gases flow to the anode and cathode side of SOFC respectively and arrives at the three-phase boundary where the electrochemical reaction occurs. The reaction within SOFC gives off heat and produces electricity at the same time. The outlet fuel containing unreacted H_2 from SOFC is burned completely in the catalytic combustor. And the exhaust gas of combustor enters the micro gas turbine to generate additional electricity. The full model of multi-energy system is established on MATLAB/Simulink platform. Several studies have been carried out on the energy system involving SOFC and gas turbine in our prvious work [16][20][21], where the modeling methodology has been verified by experimental data. Specific modeling parameters of SOFC/GT could be obtained in those literatures.

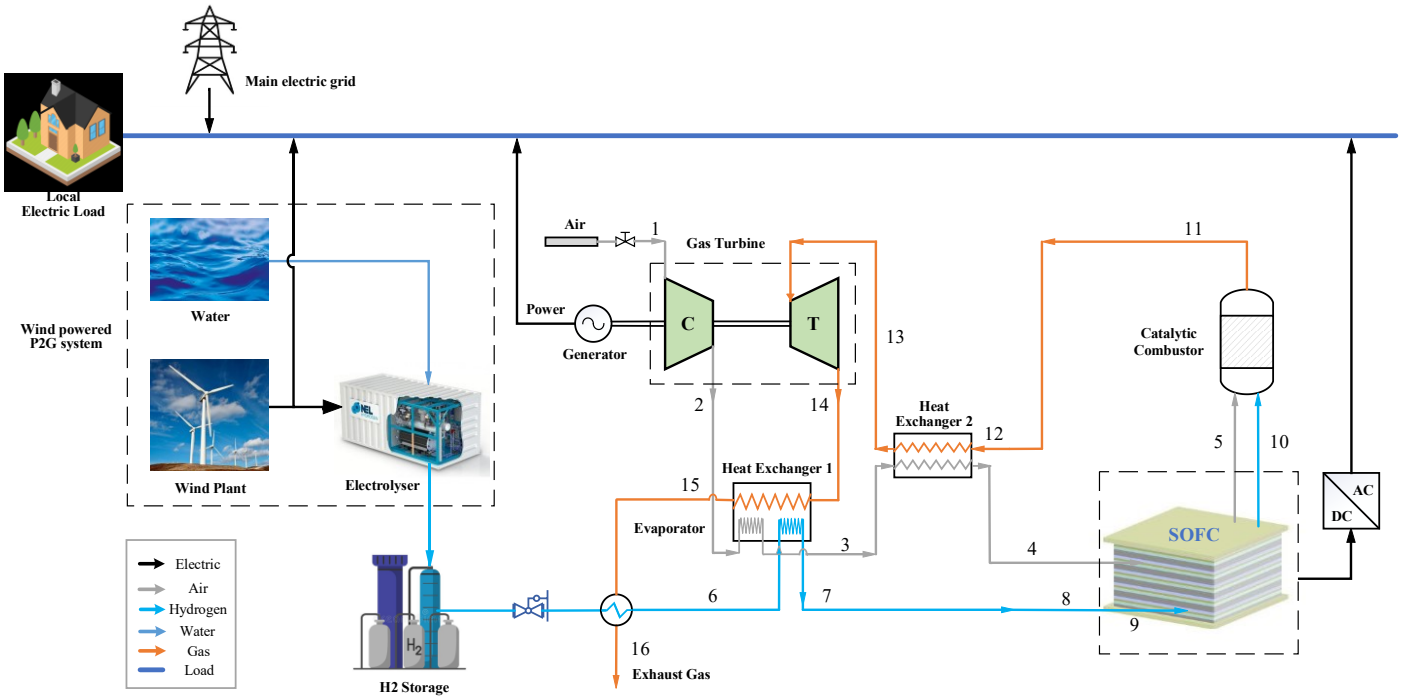

Figure 1 Layout of the integrated multi-energy system in microgrid

2.2. Renewable and demand

The characteristics of local renewable and electricity demand are essential in determining the MES capacities. Wind resource dataset from Scotland is used here [27]. With its rated capacity, the relationship between wind turbine power output and wind speed is given as follows [28]:

$$P_t = \begin{cases} P_r \dfrac{(v - v_{ci})}{(v_r - v_{ci})} & v_{ci} \le v \le v_r \\ P_r & v_r \le v \le v_{co} \\ 0 & else \end{cases} \quad (1)$$

where P_t is wind turbine output power, P_r is the rated capacity, v_{ci} and v_{co} is cut-in and cut-out speed, respectively. v_r is rated output speed and v is actual wind speed.

In this work, the peak demand in the illustrative microgrid is set as 420 kW. Demand profile is also selected from Scotland. The whole year variation of wind power level and demand is illustrated in Figure 2 with load in summer relatively lower than winter.

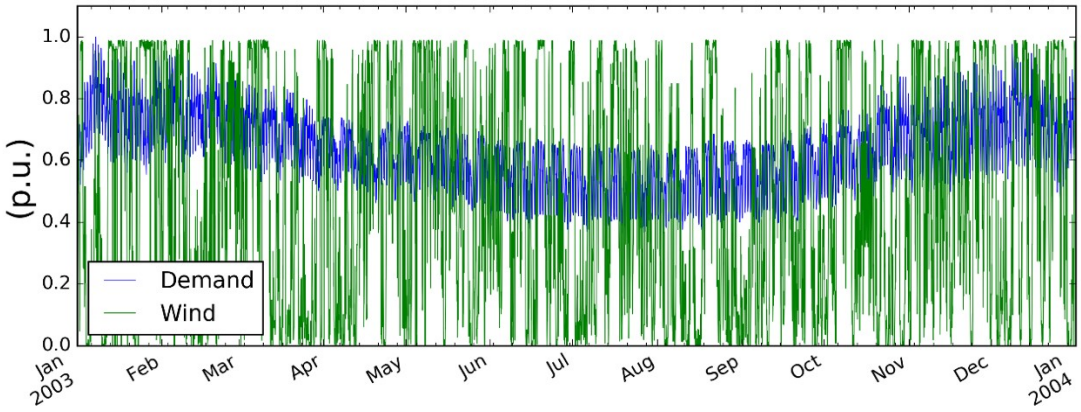

Figure 2 Annual demand and wind variation (values are provided as per unit against peak values)

2.3. Electrolyser

Electrolysers produce H_2 via the electrolysis of water powered by electricity. It is environmentally friendly when using electricity sourced from renewable energy. Moreover, it produces high purity H_2 that is favored by fuel cell systems. Different types of electrolysers are available mainly due to the different types of electrolyte material involved [29]. Among them, Proton Exchange Membrane electrolysers (PEMs) and alkaline electrolysers are popular [3].

The general efficiency of an electrolyser is defined as:

$$\eta_{\mathrm{HHV}} = \frac{M_{\mathrm{fuel}} \cdot HHV_{\mathrm{H_2}}}{P_{\mathrm{el}}} \tag{2}$$

It is predicted that the efficiency of a complete electrolyser system for 2020-2030 would be 62-82%, this paper assumed an efficiency of 75% and 0~100% operation load [16].

2.4. Storage

A storage tank is used to store the H_2 coming from the electrolyser and is connected to the fuel dispensers for SOFC/GT. The storage operates as a buffer to shift the H_2 produced at a period when wind generation is surplus to period when it becomes insufficient to demand, so as to rebalance intermittent wind energy and local electricity load. Due to the potential fluctuation of system pressure during off-design conditions, the pressures of H_2 provided by electrolyser and storages are selected as 10 bar.

2.5. Solid Oxide Fuel Cell

In this study, anode-supported solid oxide fuel cell is modelled [30]. This model has been validated with

experiment results in previous study [31]. The following assumptions are made for the SOFC [23]: 1) gas leakage in the MES is assumed to be zero, 2) only H_2 and O_2 participate in the three-phase boundary reaction within fuel cell, 3) parameters of each fuel cell in the stack are assumed to be the identical, and the outlet temperature of fuel cell is calculated as the working temperature.

In general, reactions on the anode and cathode side of SOFC are listed below:

$$H_2 + O^{2-} \rightarrow H_2O + 2e^{-1}$$

$$\frac{1}{2}\ O_2 + 2e^{-1} \rightarrow O^{2-}$$

Three types of voltage losses are considered in the model, including concentration loss, activation loss and ohm loss. The relation between cell voltage and polarization losses is as follows:

$$E(j) = E^{\mathrm{OCP}} - V_{\mathrm{act}} - V_{\mathrm{conc}} - V_{\mathrm{ohm}} \tag{3}$$

$$P_{\mathrm{SOFC}} = E(j) \cdot j \cdot L \cdot W \tag{4}$$

where V_{ohm}, V_{act} and V_{conc} represent ohm loss, activation loss and concentration loss, respectively. L and W represent the total length and width of the fuel cell stack.

The open-circuit potential (E^{OCP}) is determined by Nernst Equation, which is given as followed:

$$E^{\mathrm{OCP}} = E_0 + \frac{RT}{2F}\ln\left(\frac{p_{\mathrm{anode,H_2}}\ p_{\mathrm{cathode,O_2}}^{0.5}}{p_{\mathrm{anode,H_2O}}}\right) \tag{5}$$

where $p_{\mathrm{anode,H_2}}$ refers to the partial pressure of H_2.

Activation loss is described as the required overpotential for the fuel & air to participate in the electrochemical process in fuel cell. Here, activation loss is given by Butler-Volmer Equation:

$$j = j_{0,\mathrm{electrode}}\left[\exp\left(\frac{\alpha nF}{RT}V_{\mathrm{act,electrode}}\right) - \exp\left(-\frac{(1-\alpha)nF}{RT}V_{\mathrm{act,electrode}}\right)\right]$$

$$\mathrm{electrode} \in \{\mathrm{anode, cathode}\} \tag{6}$$

where $j_{0,\mathrm{electrode}}$ is the exchange current density and is given by the following equations, where $k_{\mathrm{electrode}}$ refers to pre-exponential factor of the exchange current density, while $E_{\mathrm{electrode}}$ represents activation energy of the exchange current density.

$$j_{0,\text{anode}} = \frac{RT}{nF} k_{\text{anode}} \exp\left(-\frac{E_{\text{anode}}}{RT}\right) \tag{7}$$

$$j_{0,\text{cathode}} = \frac{RT}{nF} k_{\text{cathode}} \exp\left(-\frac{E_{\text{cathode}}}{RT}\right) \tag{8}$$

Concentration loss is the voltage loss when mass transport effects prevent the electrode reaction in fuel cell channel [30]. On such occasion, the reactant and product concentrations at the electrode/electrolyte interfaces or three-phase boundaries (TPB) are different from those in the bulk channel flow, and the corresponding Nernst Equation is written as:

$$E_{\text{TPB}}^{\text{OCP}} = E_0 + \frac{RT}{2F} \ln\left(\frac{p_{\text{H}_2,\text{TPB}}\ p_{\text{O}_2,\text{TPB}}^{0.5}}{p_{\text{H}_2\text{O},\text{TPB}}}\right) \tag{9}$$

The difference between Eq. (3) and Eq. (7) is the concentration loss V_{conc}. Ohmic loss, representing the electric resistance due to conduction of ions and electrons among the components [32][33], is described by:

$$V_{\text{ohm}} = jR_{\text{ohm}} \tag{10}$$

$$R_{\text{ohm}} = \frac{\tau_{\text{anode}}}{\sigma_{\text{anode}}} + \frac{\tau_{\text{electrolyte}}}{\sigma_{\text{electrolyte}}} + \frac{\tau_{\text{cathode}}}{\sigma_{\text{cathode}}} \tag{11}$$

where τ_{anode}, τ_{cathode} and $\tau_{\text{electrolyte}}$ represent the thickness of the anode, cathode and electrolyte layers, while σ_{anode}, σ_{cathode} and $\sigma_{\text{electrolyte}}$ for the electronic conductivity of the anode, cathode and electrolyte, respectively [33]. During operation, SOFC safe working temperature should be maintained between 1073K and 1283K [25], meanwhile the average temperature gradient of fuel cell should be lower than 10K/cm [23].

$$T_{\text{out}} = \frac{\sum M_{i,\text{in}} c_{p,\text{i}} T_{\text{in}} + r_{\text{ele}}\left(-\triangle H_{\text{ele}}\right) - P_{\text{out}}}{\sum M_{i,\text{in}} c_{p,\text{i}} T_{\text{in}}} \tag{12}$$

For the validation of model, Fig.3 shows the comparisons of the output voltage of the SOFC with experimental date from Zhao et. al. [34]. The operation condition is set at the temperature of 800 ℃ and pressure of 1 bar. As can be seen that the difference between simulation work in the paper and results in the literature is very small, which indicates the methodology and assumption applied in the work is reasonable. Detailed results of modeling procedure could be in [30]. For safe operation, the operating temperature of fuel cell is controlled within 873-1123 K and average temperature gradient should be below 10K/cm [23].

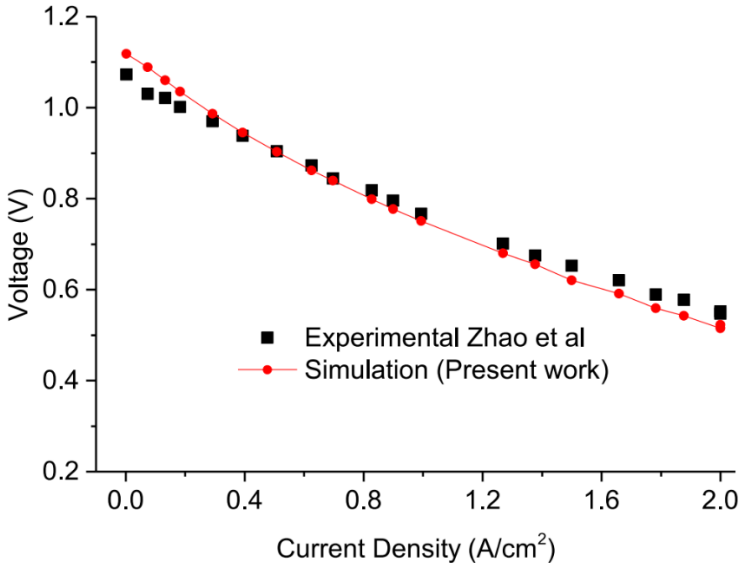

Figure 3 Validation of SOFC model with experimental results [34]

2.6. Gas Turbine

Micro gas turbine was modelled based on experimental data from a existing 30 kw-class turbine [25]. According to experiment results, the isentropic compressor efficiency is 70%–84%, and isentropic turbine efficiency presents a maximum close to 83%. The turbomachinery performance maps is considered in the MES simulation to provide the relationship between the isentropic efficiency and flowing rate, pressure ratio, as well as rotate speed. The capacity range of gas turbine for MES design is normalized based on its designed flowing rate [14]. During the simulation of a given MES, the gas turbine operates with a constant fuel/air ratio in response to the fluctuation of H_2 generated from P2G. Note that the margin surge of compressor should be kept larger than 15% to prevent damage. Meanwhile, inlet temperature of micro gas turbine (TIT) should be controlled within 1023K-1223K to protect turbine blade materials from overheat [35].

2.7. Catalytic Combustor:

Exhaust gas from the SOFC contains incompletely reacted H_2 with extremely low concentration. This part of H_2 is further utilized by catalytic combustion to improve the overall efficiency of MES [36]. The feasibility of this technology has been verified by experimental test in [37]. Combustion process is carried out in a cylindrical reactor, where the catalyst is 0.5%Pd/ZrO_2/γ-Al_2O_3 and supported in a monolithic ceramic. Experiment results reveal that 100% conversion rate was achieved for H_2, CH_4 and CO with extremely low

concentrations, which indicates the assumption applied for the catalytic combustion of MES is reasonable.

Inlet enthalpy (H_{CC}) and outlet temperature of combustor are given using as below [38]:

$$(H_{cc} + Q_{\mathrm{H_2}}) \cdot \varepsilon_{\mathrm{comb}} = \sum_m n_{\mathrm{m}} \int_{T_{\mathrm{std}}}^{T_{\mathrm{out}}} c_{p,\mathrm{m}} \mathrm{d}T \quad (13)$$

where $\varepsilon_{\mathrm{comb}}$ represents the entropy efficiency of catalytic combustor.

3. System optimization and operational strategy

3.1. Objective functions

For the task of optimizing a self-efficient MES, the primary goal is efficiently supplying the electrical demands with high local renewable but at low system cost. The efficient usage of renewables can be represented by low curtailment rate. System cost is calculated by taking into account of the capital investment and operation & maintenance cost of each system component over the lifetime. The wind curtailment rate is a function of two parts: the first part is the wasted wind power due to limit capacity of electrolyser, the second part is due to the limit capacity of H_2 storage tank. Increase the size of electrolyser and storage tank can reduce curtailment but also increase the system cost. Balancing these potentially conflicting objectives in system planning level can be easily formulated into a multi-objective optimization problem with objective functions as below, i.e., to minimum system cost (*SC*) and wind curtailment rate (*CR*) together.

$$min(SC, CR)$$

System cost is calculated using life-cycle cost (LCC) analysis as the following equation [39]:

$$SC = \sum_{i=1}^{j} CAPEX_{\mathrm{i}} + \sum_{i=1}^{j} OPEX_{\mathrm{i}} / \frac{\mathrm{r}(1+\mathrm{r})^{\mathrm{n}}}{(1+\mathrm{r})^{\mathrm{n}}-1} \quad (14)$$

where CAPEX and OPEX represent capital investment cost and annual operation & maintenance cost of wind power, P2G system, H_2 storage and SOFC/GT, respectively. *n* represents a total operation lifetime of 20 years, *r* represents the discount rate, which is selected as 8.9% in this study [40]. The cost parameters of each

component in the multi-energy system are given in Table 3, and the annual operation & maintenance cost of SOFC/GT is set as 6% of its total CAPEX [41].

Wind curtailment rate is given as the percentage of curtailed wind power in the overall wind power generated. In the proposed MES, all remaining wind output after meet electricity demand will be converted to hydrogen by P2G and stored for a later time. Therefore, the total curtailed wind power can be split into the parts due to capacity limits of P2G electrolyser and H_2 storage. Given that calculation of curtailment rate is based on timely data monitored by Simulink, the equation below is presented to introduce the concept of CR:

$$CR = \frac{\sum_t Wind_{\text{wasted,P2G}} + \sum_t Wind_{\text{wasted,storage}}}{\sum_t Wind_{\text{total}}} \quad (15)$$

In this multi-objective optimization, the installed capacity of wind power, capacity of electrolyser, capacity of H_2 storage, SOFC fuel cell number, utilization ratio and gas turbine capacity are formulated as design variables to be optimized. Considering the peak demand of 420 kW in the system and the also development level of selected technologies [21], the ranges of above design variables have been given in Table 2.

To guarantee high level of wind power usage, the overall renewable energy penetration level (REP) is included in the optimization problem as a constraint [14]. In the case study, REP is defined by the following equation and REP^+ is set at 0.9:

$$REP = \frac{\sum_t W_{\text{wind,t}}}{\sum_t (W_{\text{wind,t}} + W_{\text{grid,t}})} \quad (16)$$

$$REP \geq REP^+ \quad (17)$$

Table 2 Optimization range of design parameters

Design parameters	Variation range for optimization
Wind plant rated power	400 ~ 1000 kW
Electrolyser power capacity	100 ~ 2000 kW
Storage mass capacity	100 ~ 2000 kg
SOFC cell number	900 ~ 1200
SOFC utilization ratio	0.7 ~ 0.85
Gas turbine modeling factor	1.3 ~ 1.5

Table 3 Economic cost for each component of multi-energy system

Components	Investment and O&M cost of multi-energy system	Literature source
Wind power	CAPEX=1750 £/kW, OPEX=3%	[42]
Power-to-gas	CAPEX=1015 £/kW, OPEX=2.75%	[29]
Storage	CAPEX=310 £/kg, OPEX=1%	[43]
SOFC stack	$Z_{\mathrm{SOFC}} = A_{\mathrm{a}} \times N_{\mathrm{SOFC}} \times (2.96 \times T_{\mathrm{SOFC}} - 1907)$	[44]
Air Compressor	$Z_{\mathrm{AC}} = 91652 \times (W_{\mathrm{AC}}/455)^{0.67}$	[36]
Fuel Compressor	$Z_{\mathrm{FC}} = 91652 \times (W_{\mathrm{FC}}/455)^{0.67}$	[45]
Gas turbine	$Z_{\mathrm{GT}} = \left(\frac{479.34 m_{\mathrm{g}}}{0.92 - \eta_{\mathrm{GT}}}\right)\left(\mathrm{Ln}\left(\frac{P_{\mathrm{inlet}}}{P_{\mathrm{outlet}}}\right)\right)(1 - \mathrm{e}^{0.036 T_{\mathrm{inlet}} - 54.4})$	[46]
Afterburner	$Z_{\mathrm{AB}} = \left(\frac{46.08 \times m_{\mathrm{g}}}{0.995 - \left(\frac{P_{\mathrm{AB,outlet}}}{P_{\mathrm{AB,inlet}}}\right)}\right) \times (1 + \mathrm{e}^{0.018 T_{\mathrm{AB}} - 26.4})$	[35]
AHX	$Z_{\mathrm{AHX}} = 3 \times 130 \times (A_{\mathrm{AHX}}/0.093)^{0.78}$	[47]
FHX	$Z_{\mathrm{AHX}} = 130 \times (A_{\mathrm{FHX}}/0.093)^{0.78}$	[38]
Inverter	$Z_{\mathrm{inv}} = 100000 \times (P_{\mathrm{SOFC}}/500)^{0.7}$	[35]

3.2. Two-level modeling approach and optimization algorithm

The decision-making structure involved in the problem of optimally planning and also operating the system can be accommodated in a two-level model, which splits the optimization into (upper) planning level and (lower) operational level, representing decisions that need to be made pre and after a certain design is revealed, respectively. The final decision-making is determined by the overall performance of both levels.

The two-levels structure for optimizing the specific integrated energy system studied here is modeled and

solved using Genetic Algorithm. Genetic algorithm is an iterative and global search method that imitates biological evolution to find optimal solutions to a given problem [74]. The main structure can be represented using the diagram shown in Figure 4.

Upper level: planning MES capacities:

The upper level of the optimization is established to find the optimal configurations with the minimum total annual cost and maximum penetration level. The decision variables are the capacities of the MES components, namely the selection and sizing of wind turbine, capacity of electrolyser, H_2 storage, SOFC fuel cell number, gas turbine capacity and fuel/air ratio that should be installed in the system. In this work, the configuration design is implemented using the GA toolbox *gamultiobj* in MATLAB and coupled with lower level operational model in Simulink for simultaneously optimizing system design with thermodynamic operational modeling. Based on the ranges of design parameters given in Table 1, GA generates an initial group of candidate designs (i.e., the first generation of populations) and then continuously evaluates and updates these candidates through the standard sorting, crossover and mutation procedures as shown in Figure 4. The population size, crossover probability, elite fraction, mutation probability and maximum generation are set as 100, 0.8, 0.05, 0.01 and 200, respectively.

After evaluating the candidates in lower level, the fitness values are returned and collected for comparison. This iterative procedure will be repeated for the 100 population in the maximum generation of 200. Finally, individuals with the best fitness (above a certain threshold) is selected. The total annual cost and wind curtailment rate of the selected system configurations will be given in Pareto front, which presents the solutions of multi-objective optimization.

Lower level: evaluating the operation of given MES

The lower level contains the MES model developed in Simulink, which is based on the component models in Section II. The MES is simulated with the objective to reduce the wind curtailment at each period.

The decision variables here refer to the operating patterns of the selected component, such as the amount of wind used for local demand and electrolysis, H_2 charged/discharged in storage and generation level of SOFC and gas turbine at each timestep. The overall system performance is evaluated in three steps. In Step A, design parameters of MES components are collected from GA population to establish an MES candidate with hourly wind power and electric demand data. In Step B, the operation of MES candidate is simulated with the given power management strategy (details in Section 3.3). Power management strategy is designed to improve the cascaded utilization of wind power, and it is subject to a range of constraints, such as the capacities and safety ranges given at the planning level. In the safety range detection module, multiple safety criteria are checked as constraints, including SOFC operating temperature, SOFC temperature gradient, gas turbine inlet temperature, compressor surge margin, etc. In Step C, system performance values, i.e., the total operational cost and overall wind curtailment rate, are summarized back to GA as the fitness value of given candidate.

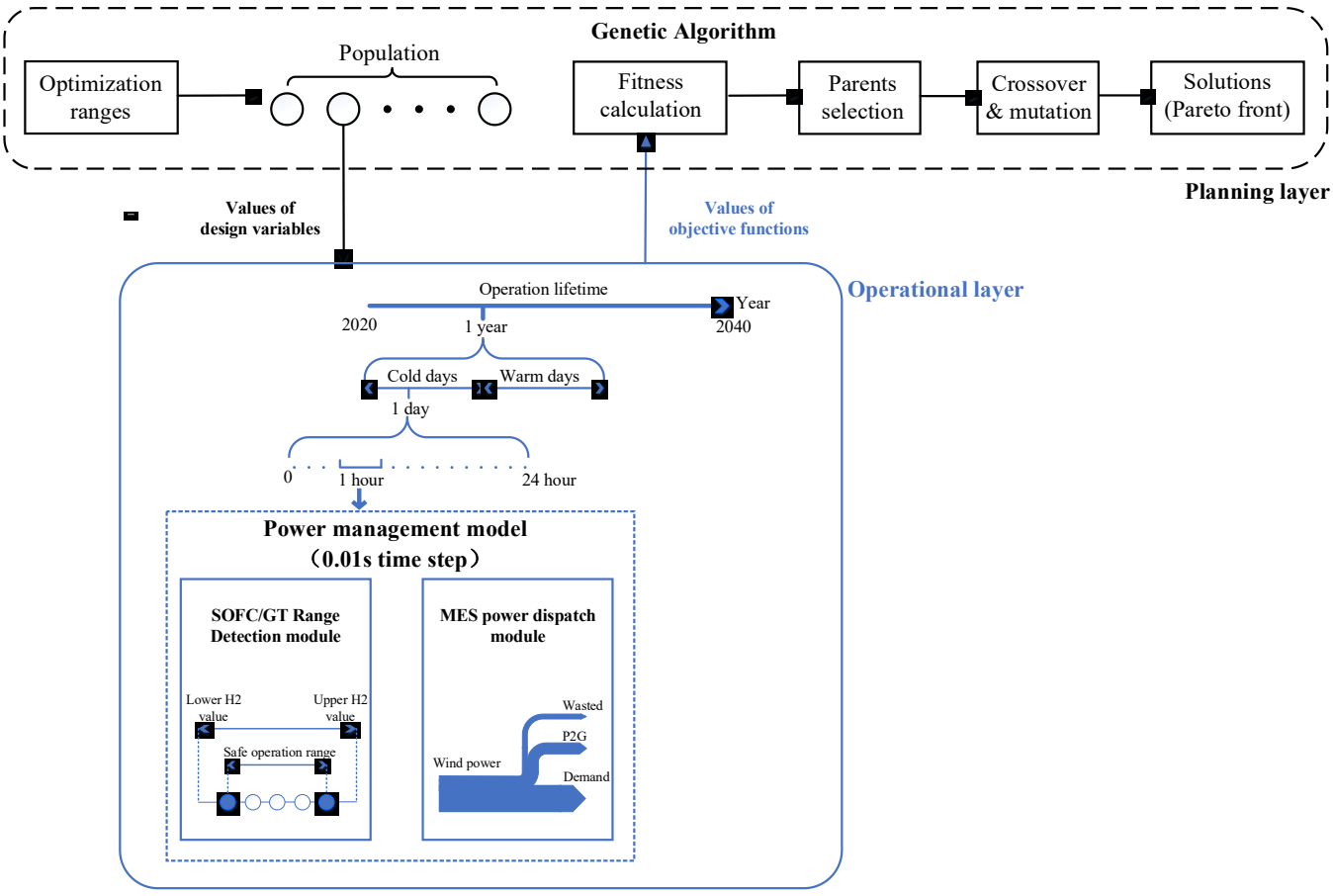

Figure 4 Two-level optimization approach of the system

Through the two-level optimization structure, as shown in Figure 4, the long-term planning and short-term operational models are coupled together at multiple time scales. The overall planning lifetime of multi-energy system is 20 years. At the target year, the operation of the system is considered with hourly variations of wind power and electricity demand. Inside the hourly simulation, with the detailed thermodynamic model of SOFC/GT running at the time step of 0.01s, 500 iterations are taken to reach the convergence. Performance characteristics of the illustrative system at steady state can be determined in less than 3 minutes (140.94 s) in response to the varying wind and demand.

3.3. Power management strategy

For evaluating the system design, a power management strategy is proposed to efficiently operate the system and improve the utilization of renewable energy. The aim of the strategy is to ensure that local demand in microgrid is satisfied at any time; meanwhile SOFC/GT, electrolyser and H_2 storage tank could always operate within acceptable safe ranges. The full logical schematic of the strategy is given in Figure 5, which detailly presents the dispatch of multiple energy flows in response to wind power and local demand variation. Although there are many judgment modules that represent the technical and safety limits in the schematic figure, the basic operation principles can be summarized as threefold:

a) local demand is met first using local wind power subject to its availability; if there is excess wind, it will be used in P2G.
b) the remaining demand is supplied by the SOFC/GT;
c) electricity from main grid is only used as the last resort for demand.

These principles maximize the utilization of available wind power, with SOFC/GT as flexible supply to fill gap when wind power is not enough. Grid supply is included as a last resort and the total amount of imported electricity is limited by REP, which could guarantee high self-sufficiency of renewables given that SOFC/GT is also indirectly fueled from the excess wind.

Based on these principles mentioned above, the detailed procedure of system behavior strategy in Figure is given as below:

1) Importing design parameters from upper level GA module to the controller at time t.

2) In the SOFC/GT range detection module, max & min load limits and corresponding H_2 flowing rates of SOFC/GT are calculated and saved.

3) Compare the wind power and local demand at time t.

Condition 1: Wind power is enough to support the demand, then use the excess wind power for P2G plant.

Condition 2: Wind power is not enough for local demand, then calculate the load gap ($gap = demand - wind\ \ power$).

Analyze if the gap is within the available range of SOFC/GT.

Condition 2.1: The gap is within the operational range, then use SOFC/GT to support the gap.

Condition 2.2: The gap is lower than the min power of SOFC/GT. Operate SOFC/GT at min power output to fully support the demand, use wind power to eliminate the new gap ($gap = demand - SOFC/GT\ min\ power$). If excess wind power is left, use it for P2G.

Condition 2.3: The gap is higher than the max power of SOFC/GT. Operate SOFC/GT at max power to fully support the demand, transport additional electricity from main grid to eliminate the new gap ($gap = demand - wind\ \ power - SOFC/GT\ max\ power$).

4) Calculate the H_2 input and output at time t, and check the amount of new H_2 storage ($H2\ \ storage = initial\ \ H2\ \ storage - H2\ \ output + H2\ \ input$).

Condition 1: H_2 amount is within the storage capacity, update the data to time t+1.

Condition 2: H_2 storage in the tank will be full filled. Curtailment the excess H_2 and calculate the

corresponding wind power wasted.

Condition 3: H_2 storage in the tank will be used up. Calculate the additional electricity needed from main grid for support.

5) Operation of the system at time t is completed, import design parameters to power management controller at time t+1, return to Step 1) and continue.

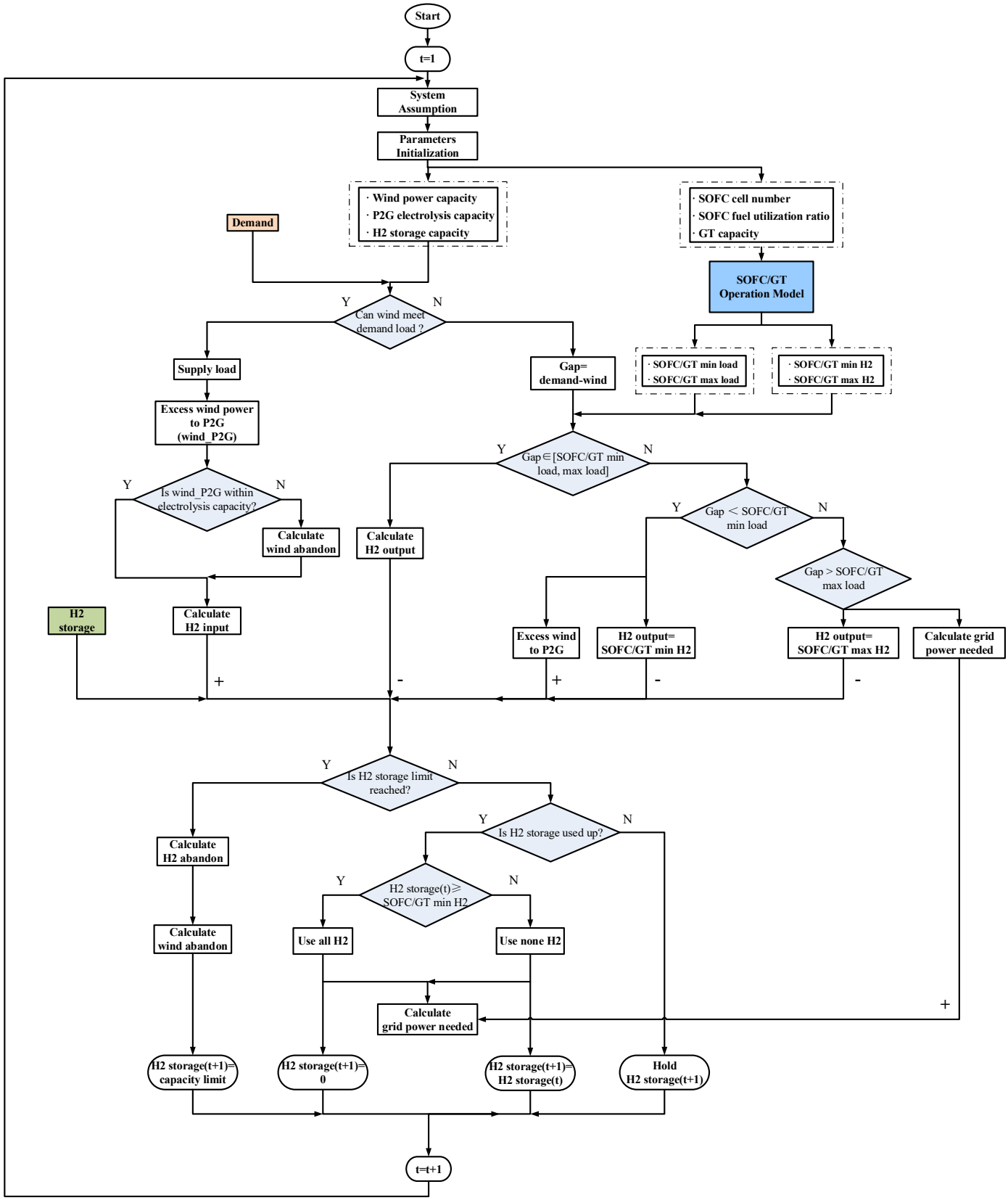

Figure 5 Logical schematic of power management strategy

4. Case Study

In this study, the multi-energy system is designed to be highly self-sufficient to demand using local wind

resources. The demand in the case is peak at 420 kW. Demand and wind profile in Scotland were used. Two typical weeks in January and July are selected to represent winter and summer scenarios, respectively. To ensure high self-sufficiency, the minimum value of REP is set as 0.9.

The optimal design solution was identified by the formulated optimization process as Pareto front, as given in Figure 6. Note that the multi-objective optimization does not just provide a single optimal. Instead, a series of solutions are provided in Pareto front and are considered mathematically equal. In Figure 6, as the wind curtailment rate decreases, the corresponding system cost for the MES rises up significantly, representing a clear trade-off between these two objectives. A certain point in the black is selected as an example for system study, where the optimal design decisions are listed in Table 4. The optimum configuration for the selected system consists of 693.5 kW wind turbine, a 319.5 kW PEM electrolyser, 211.8kg hydrogen tank, 962 SOFC cell units with 0.816 SOFC utilization ratio and 33.5 kW gas turbine. In practice, the selection of design will be subject to the preferences of the decision-maker and manufacturer, which could be different due to specific conditions.

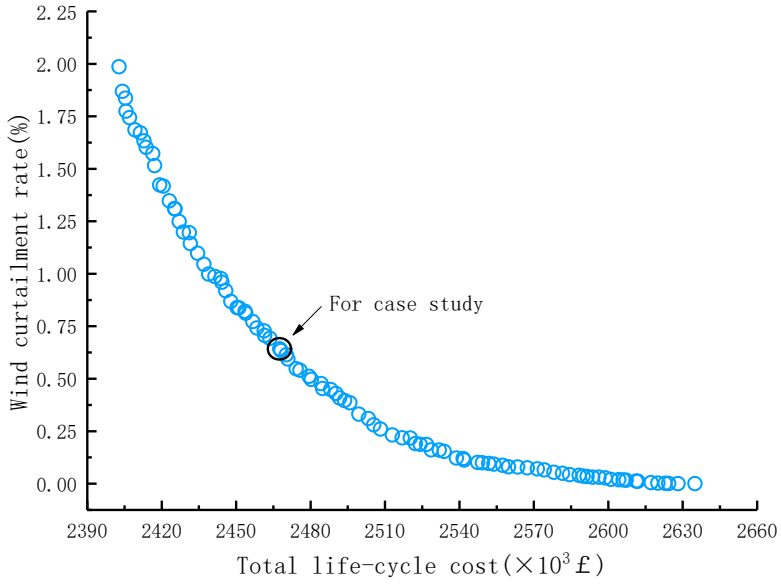

Figure 6 Pareto front for a selected case of multi-objective optimization

Table 4 Design parameters of system under selected case

Design parameters	Wind power capacity	Electrolyser capacity	H_2 storage capacity	SOFC cell number	SOFC Utilization ratio	Gas turbine capacity factor
Values	693.5 kW	319.5 kW	211.8 kg	962	0.816	1.44

4.1. Results and discussion under the selected case

Performances of MES under the selected case are given in Table 5. Under the optimal configuration, the system operates with LCC of £2,468,093 and wind curtailment rate of 0.63%. The penetration level of wind power is 90.06%, indicating the majority of electric demand is supported by renewable. Meanwhile, electrical efficiency of SOFC/GT reaches as high as 67.1% within safety constraints. These results indicate that primary purpose of MES is achieved and that the multi-objective optimization methodology is reasonable.

Table 5 Overall performances of multi-energy system under selected case

Parameters	**Value**
Life-cycle cost (LCC)	£2468093
Wind curtailment rate	0.63%
renewable energy penetration level (REF)	90.06%
SOFC/GT maximum efficiency	67.1%

The hourly variation of electricity supply in MES during winter and summer weeks are given in Figure 7. The operation of wind power, SOFC/GT, P2G plant and main grid electricity are controlled by the logical schematic of system behaviors mentioned above. Compared between seasons, the peaks of wind power and electricity demand are both lower in summer, which is typical condition in Scotland. Additional electricity from main grid is applied in both winter and summer scenarios. Note that the case study presented here is a result of optimization from perspectives of economic and wind curtailment issues.

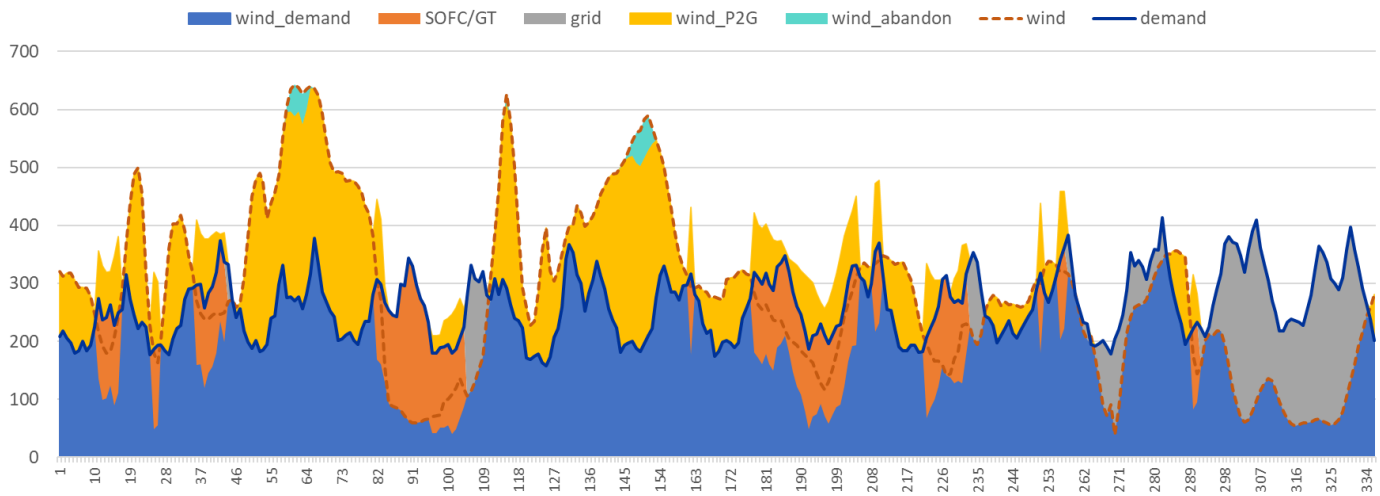

(a)

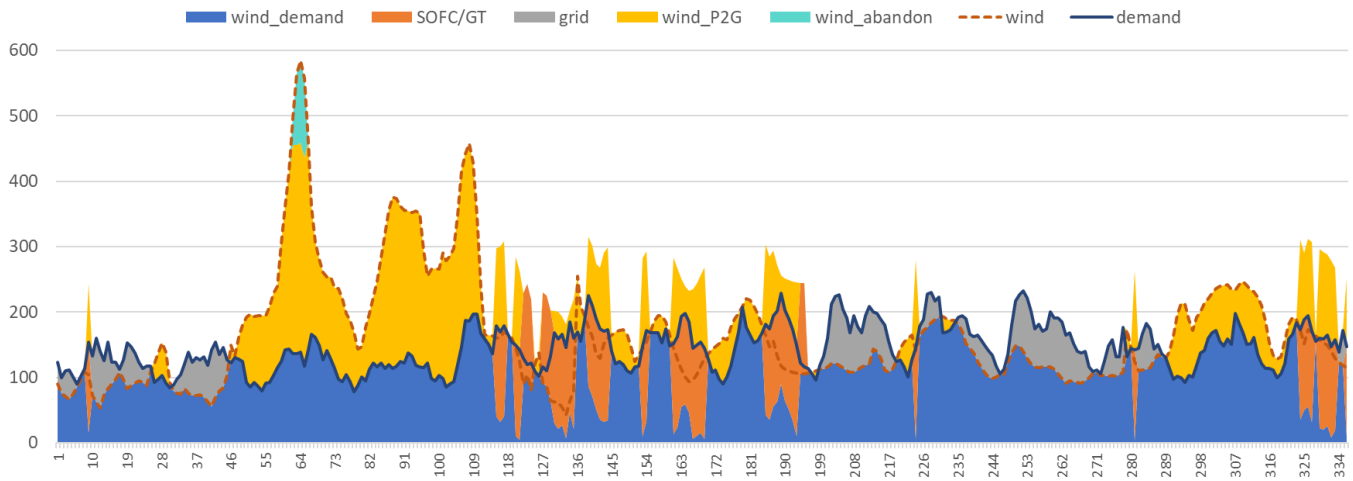

(b)

Figure 7 Electric supply and demand balance of MES in winter (a) and summer (b) scenarios

The detailed distribution of wind power in the winter and summer scenarios is illustrated in Figure 8. As can be seen that, wind power from the integrated system is divided into three parts: wind power for supporting electricity demand, wind power for P2G process and wind power for curtailment. Percentages of three types of wind power along the two-weeks' operation are given in the figure. According to the results, 66.36% of overall wind power in the scenarios are used for electricity demand, 33.01% of wind power is provided to electrolyser for P2G, and the left curtailment wind power is only 0.63%. During most operating hours, most of the wind power is used for supporting local demand. However, the percentage of wind for P2G process

could be very high in a few hours, reaching a maximum of 73.5% in winter and 97.1% in summer. Therefore, only a small part of wind power is wasted during winter and summer operation, indicating the optimization method and power management strategy of the multi-energy system in this paper are effective.

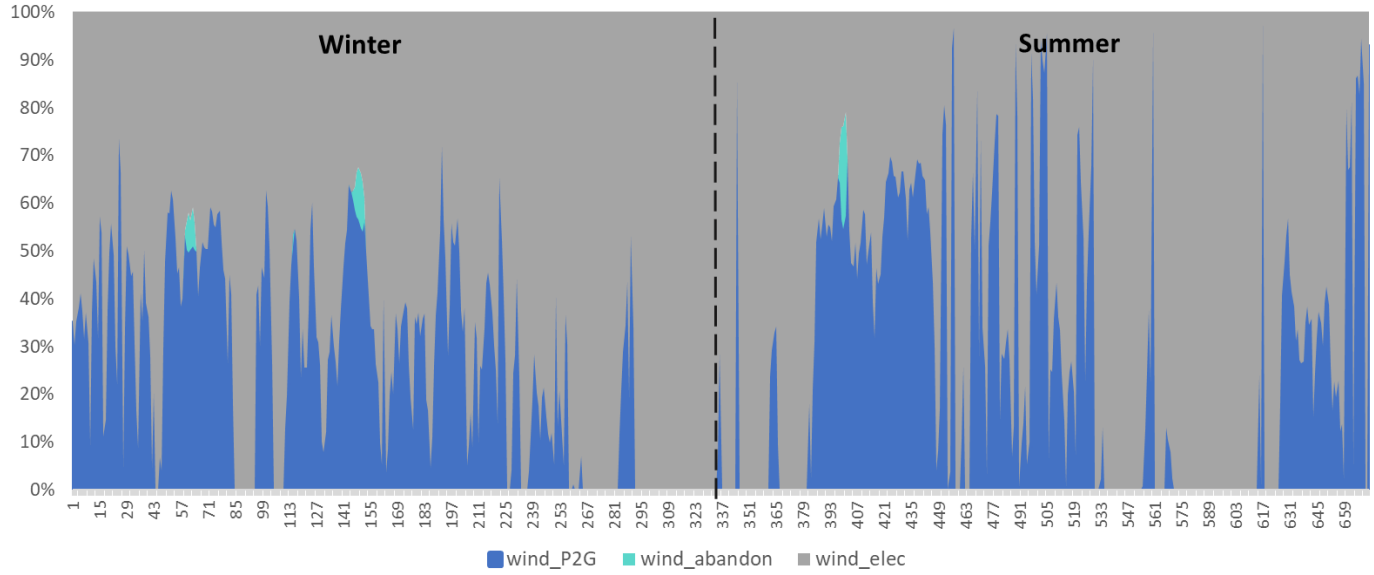

Figure 8 Percentages of wind power for multiple uses during system operation

The capital investment percentage of each component is shown in Figure 9. It is clear that investment cost of wind power is the highest among all the components. Wind power plant makes up 68.35% of the total investment, with P2G system occupies 18%. SOFC/GT and H_2 storage facility make up 8.7% and 4.95% of the total cost, respectively. Note that the investment cost percentage of SOFC/GT is only about half of P2G. This might indicate that in the optimal configuration, SOFC/GT could be an economically competitive part of the integrated renewable energy system, even though the technology is still considered expensive.

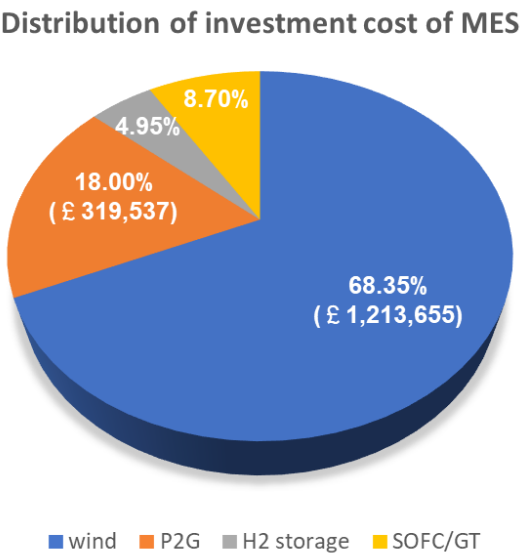

Figure 9 Capital investment breakdown of MES components

4.2. Operation characteristic of integrated multi-energy system

In order to analyze the operation of each component in the integrated multi-energy system under the selected case, the hourly operation of each induvial competent such as wind power, local demand and H_2 storage is given in Figure 10. In Figure 10 (a) and (b), curves of wind power power and electricity demand are shown in winter and summer scenarios. It can be seen that the maximum peaks of wind power during two seasons are not much different, with the value of 643.6 kW and 584.6 kW, respectively. However, the fluctuation range of wind power in winter is much stronger than that in summer scenario. The average value of local demand is also higher in winter due to the increase in electricity consumption in house heating, etc.

Figure 10 (c) and (d) show the distribution of wind power power along the operating hours. As can be seen that for the most time in winter, the amount of wind power for local demand is higher than other uses, with a peak value of 377.91 kW. Major wind curtailment issue happens at the 61-66nd hour and 146-154th hour; at the same time, wind power for P2G meets the capacity limit of electrolyser and thus keeps constant. For summer operation in Figure 10 (d), although the amount of wind power for demand is also higher in most conditions, its peak value decreases to 207.2 kW. Stronger wind curtailment occurs in summer scenario, with its maximum value reaching as high as 126.2 kW.

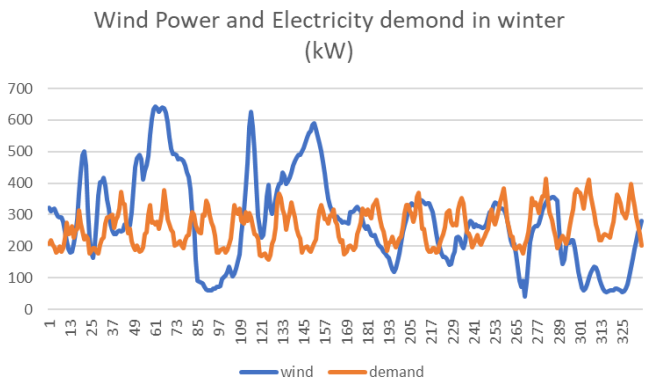
Wind Power and Electricity demond in winter (kW)
wind
demand

(a)

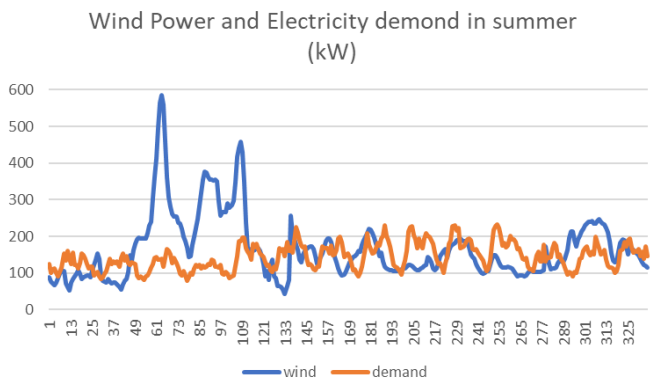
Wind Power and Electricity demond in summer (kW)
wind
demand

(b)

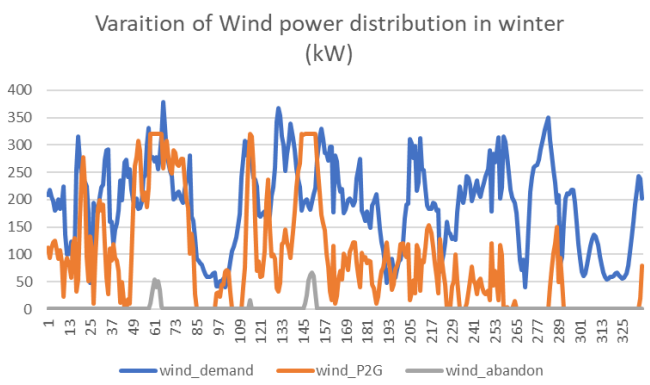
Varaition of Wind power distribution in winter (kW)
wind_demand
wind_P2G
wind_abandon

(c)

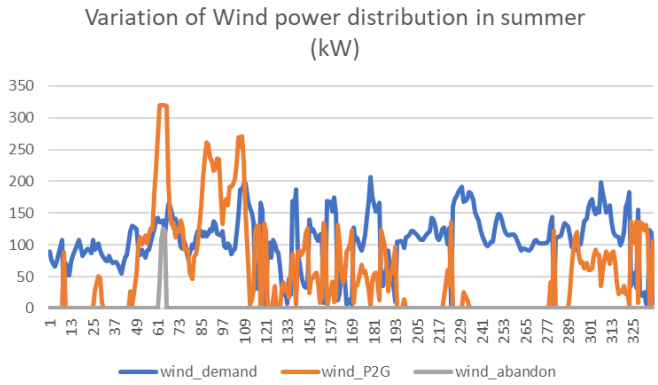
Variation of Wind power distribution in summer (kW)
wind_demand
wind_P2G
wind_abandon

(d)

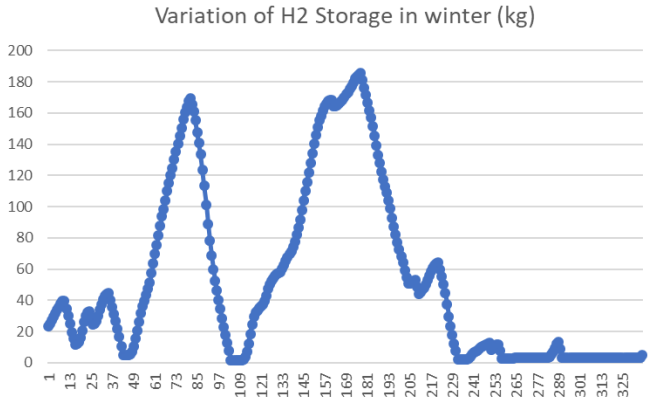
Variation of H2 Storage in winter (kg)

(e)

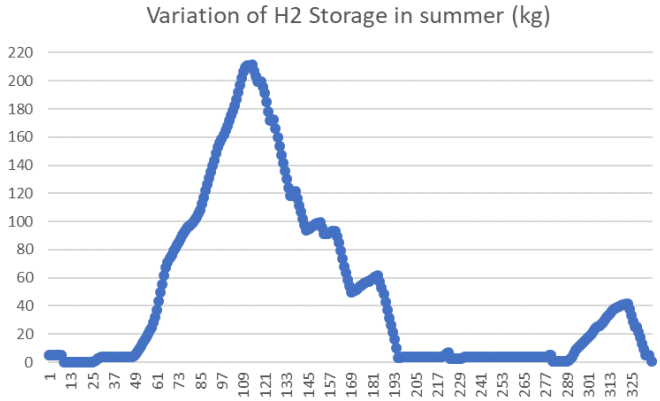
Variation of H2 Storage in summer (kg)

(f)

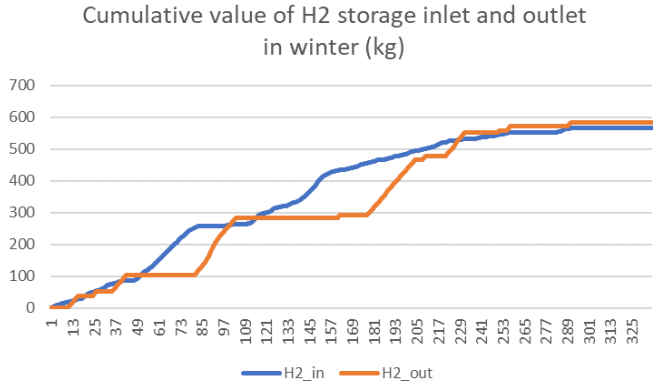
Cumulative value of H2 storage inlet and outlet in winter (kg)
H2_in
H2_out

(g)

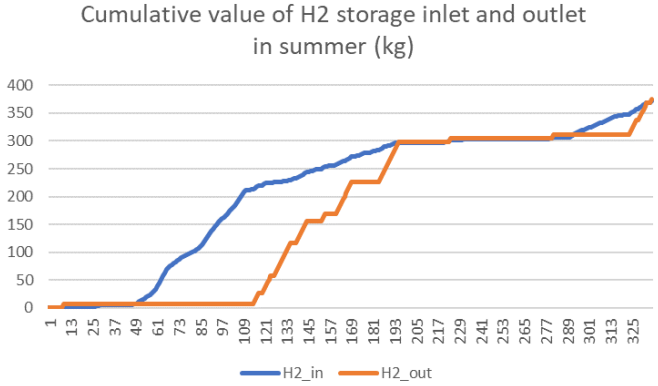
Cumulative value of H2 storage inlet and outlet in summer (kg)
H2_in
H2_out

(h)

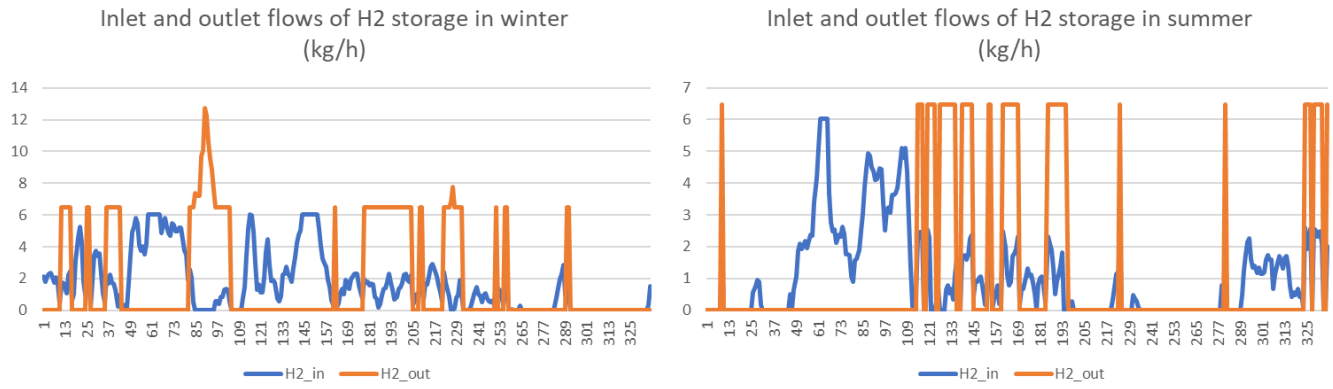

(i) (j)

Figure 10 Variations of wind power, P2G and storage in multi-energy system

Variations of H_2 storage during winter and summer scenarios are given in Figure 10 (e) and (h). The initial amount of H_2 in the tank is set as 10% of the maximum capacity. In Figure 10 (e), two major peaks of H_2 storage are captured at the 84th hour and 178th hour, with the maximum value of 185.5 kg. Only one peak value occurs in summer scenario with the value of 211.5 kg, very close to the capacity limit of 211.8 kg. The values of H_2 storage at the beginning and end of each scenario are close to the other, which indicates full circulation in the typical weeks and is representative of long-term operation.

It can be seen that the charging/discharging slope of H_2 storage near its turning point is very sharp and close to a linear tendency. To analyze this issue, the cumulative amounts of H_2 input and output of storage tank are monitored and shown in Figure 10 (g) and (h). Firstly, the H_2 input comes from wind-powered P2G, while the H_2 output comes from operation of SOFC/GT. It can be clearly seen that the cumulative value of H_2 input is increasing smoothly both in Figure 10 (g) and (h). However, the cumulative value of H_2 output is changing linearly for most hours. The only reason for this situation is that SOFC/GT is operating at its boundary point and consumes a constant volume of H_2, and this is proved in Figure10 (i) and (j). Furthermore, the consuming rate of H_2 of hybrid system is much higher than the generating rate of H_2 by P2G process, which is clearly shown in Figure 10 (h). The correlation between these factors results in the variation of storage in the figure.

Figure 11 (a) and (b) illustrate the operation hours of P2G system and SOFC/GT during the study period.

In both scenarios, P2G system generally operates for longer hours than SOFC/GT. There are certain days when the operation of both SOFC/GT hybrids and P2G unit were seen. The electrolyser generates H_2 nearly every day, and there are six days in winter and five days in summer when P2G unit operates for 24 hours. This frequent operation of P2G significantly contributes to the decreasing of wind power curtailment and improves the flexibility of the integrated MES.

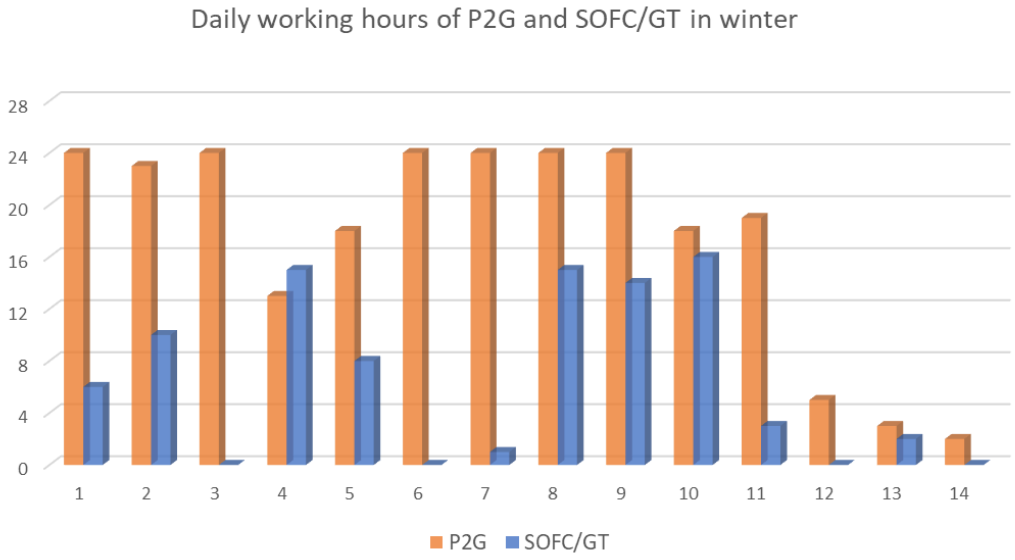

(a)

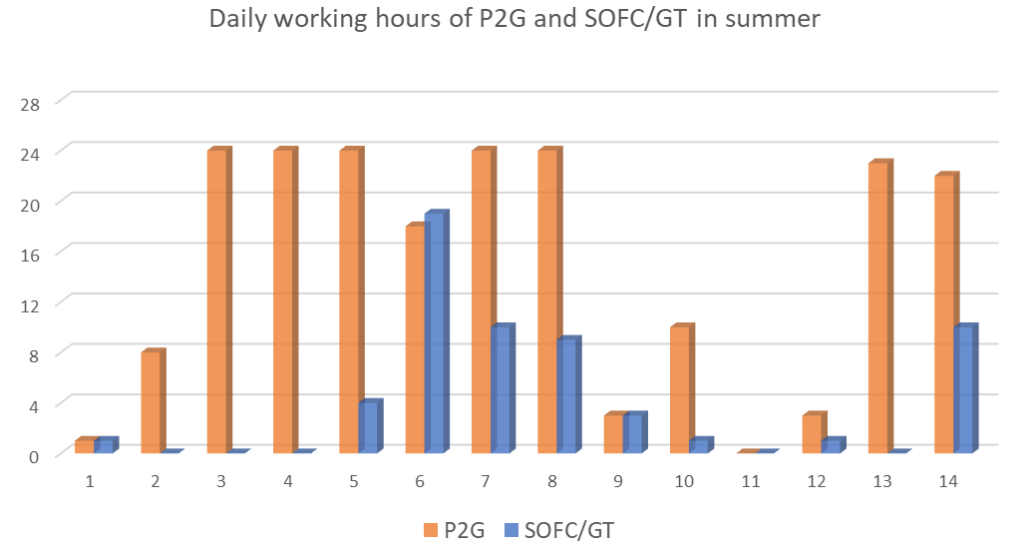

(b)

Figure 11 Daily working hours of P2G and SOFC/GT in winter (a) and summer (b)

4.3. Parametric sensitivity analysis

The sensitivity study is carried out first to analyze the impact of correlation between wind power plant and electrolyser capacity on the performance of MES. Variations of wind curtailment rate and REP under different combination of these two parameters are presented in Figure 12 (a) and (b). It can be seen in Figure 12 (a) that, wind power capacity increase with higher targeted level of REP, indicating more wind power is used in the multi-energy system. Basically, 90% REP is achieved with a wind capacity of 700 kW. As wind capacity rises higher than 800 kW, the increasing rate of REP gradually slows down. This diminishing marginal utility indicates that increasing renewable penetration of energy system to 100% requires much larger wind power scale, which could result in rapidly increasing investment cost. Compared with wind power, the influence of capacity of electrolyser on REP is much smaller. Especially when the electrolyser capacity is higher than 200 kW, its influence on REP is significantly wakened.

The combined effects of wind power capacity and electrolyser capacity on wind curtailment rate are given in Figure 12 (b). As wind capacity increases, the wind curtailment rate amount first keeps stable and then rises up sharply. This is because then excess wind power is consumed by electrolyser and P2G process. The turning point occurs as the scale of wind power increases to 700 kW, where the electrolyser quickly meets its capacity limit and in turn results in an increase of wind curtailment. In Figure 12 (b), the capacities of wind power and electrolyser both leave major impacts on wind curtailment issues. If the capacity limit of P2G is set smaller than 100kW, the wind curtailment rate rises sharply could happen even with a small wind power scale. This indicates that the correlation and matching of these two facilities need to be carefully settled with considerations of wind utilization and investment cost.

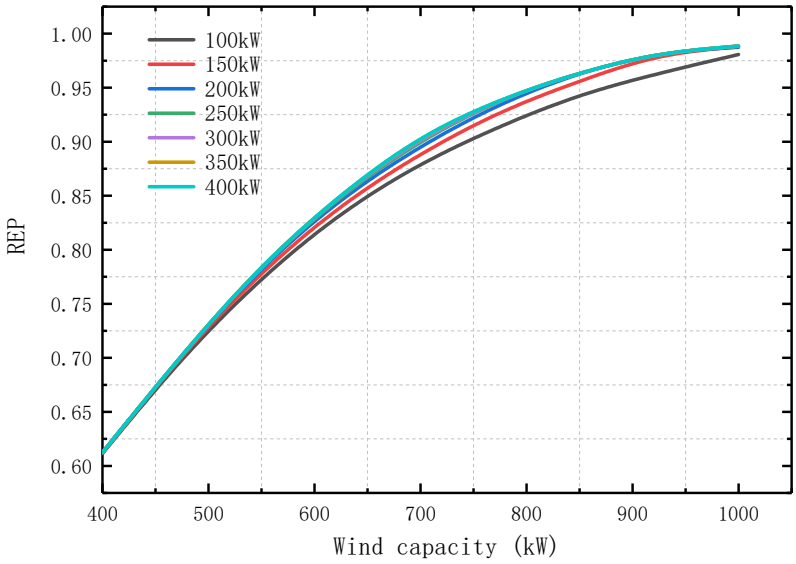

(a)

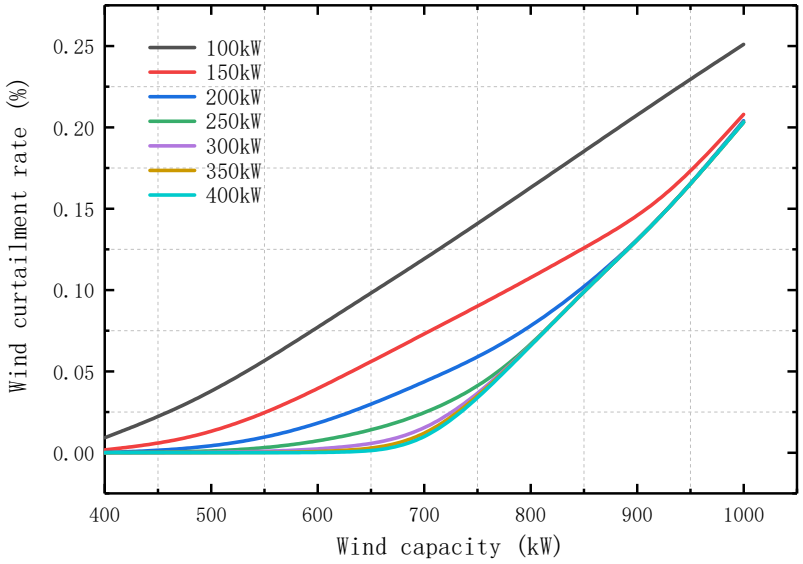

(b)

Figure 12 Effect of wind power capacity and P2G capacity on wind annual rate and REP

Figure 13 presents the sensitivity analysis of each key configuration parameters on the performance of MES. Here, the testing range of each parameter is between 80% to 120% of the optimal value in Table 3, and the results of LCC, REP and wind curtailment rate are given as relative values against these found in the optimal configuration in Table 4. The filled bars represent the values caught between the 25% and 75% of parameter ranges. As can be seen that, variation of wind power capacity leaves the largest impact on overall MES performances, resulting in LCC, REP and wind curtailment rate increasing up to 108.6%, 106.5% and

14 times of the optimal values, respectively. Especially the wind power curtailment rate is most sensitive to the installed capacity, with its value varying from 0.6% to 8.7%. This feature is also clearly shown in Figure 12 (b) as the wind curtailment witnesses sharp increasing. This result indicates that the scale of renewable generation is the primary issue to be settled for the design of MES system.

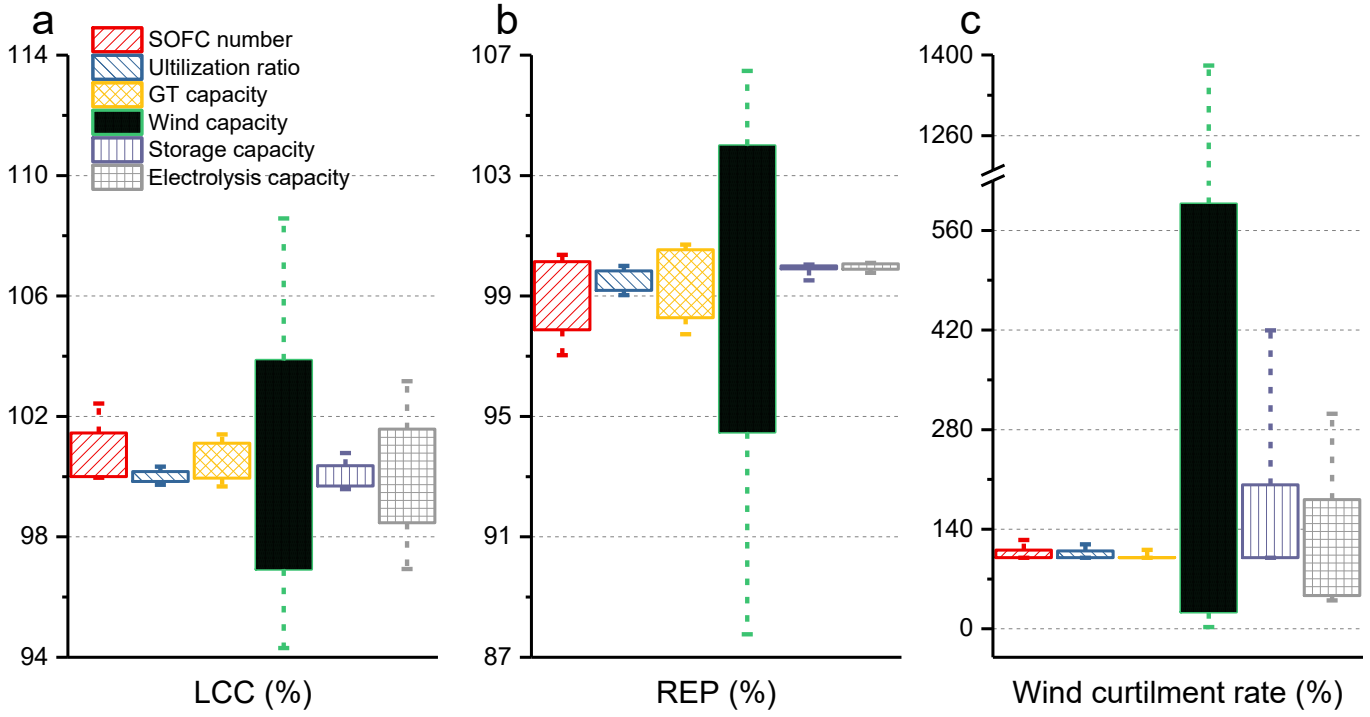

Figure 13 Sensitivity analysis of optimized variables on the performance of MES

By comparing Figure 13 (b) and (c), it is found that SOFC/GT parameters (stack number, utilization ratio and GT capacity) have more significant effect on the value of REP than P2G parameters (electrolysis and H_2 storage). However, in Figure 13 (c), variations of P2G parameters results in higher level of fluctuations of wind curtailment rate. This could be explained by the operating mechanism and roles of MES components: the scale of SOFC/GT determines how much H_2 could be finally utilized and so directly related to the overall penetration level of renewable wind (REP); the capacity of P2G determines how much excess wind power could be captured and transferred to H_2 for downstream components, which directly effects wind curtailment rate. The sensitivity analysis reveals the influences of each configuration parameter on MES performances in

different levels, which could improve the understanding of such system and benefits manufactures in design and optimization.

5. Conclusions

This paper presents a multi-energy system based on wind power, electrolyser, H_2 storage and SOFC/GT. A two-level multi-objective optimization method involving multiple time scales is carried out with regards to wind curtailment rate and total life cycle cost. In this approach, genetic algorithm (GA) operates in the planning layer and is coupled with a simulation model based on thermodynamic wind/P2G/SOFC/GT model in the operational layer. In response to the fluctuations of wind power and demand, a power management strategy is coupled in the simulation model to realize the coordinate operation of critical components. Through simulation and optimization, the main conclusions could be as follows:

1) The case study is carried out in winter and summer scenarios, and optimization results show that under the selected case, the multi-energy system could reduce wind curtailment rate to 0.63%, with renewable energy penetration of the system reaching a high level of 90.1%, which indicates the effectiveness of the proposed system configuration and two-level optimization methodology.

2) The optimized LCC of multi-energy system is £2468093, with wind power making up 68.35% of total capital investment. SOFC/GT cost only half of P2G, and could operate under the maximum electrical efficiency of 67.1% with multiple safety constraints satisfied. These results clearly indicate the economic and technical feasibility of SOFC/GT in a renewable-powered P2G system.

3) The operation hours of P2G count for 67.3% of the whole simulation period. The operation pattern of electrolyser under the power management strategy present a daily-continuous style rather than a intermittent style. This long-term operation significantly contributes to the elimination of wind power curtailment and improves the sustainability and reliability of the integrated multi-energy system.

4) Sensitivity analysis indicates that wind capacity has the strongest impact on REP of system among all

the optimized parameters. Meanwhile, the influences of these design parameters on wind curtailment rate are coupled with each other. With the electrolyser capacity reduced from 400 kW to 150 kW, the turning point for wind power capacity changes from 700kW to 400kW, where wind curtailment rate witnesses a sharp increase.

Overall, the proposed MES system has high cascaded utilization of renewable energy by coupling wind generation with P2G and SOFC/GT. With appropriate configuration design, SOFC/GT has relatively small size and run at high efficiency level with multiple safety constraints satisfied. While the optimal configuration depends on the local demand and renewable profiles and need to be investigated on a case-by-case basis, the proposed system model and two-level integrated optimisation method can be used by power system designer as general framework for assisting the design process. The application scenarios of this promising MES could be extended from grid-connected system to off-grid, such as island locations, where a diesel backup generator could be added to the system to achieve a complete stand-alone mode. In future works, modeling complexity of electrolyser and storage tank could be further improved with additional safety constraints considered. Although this study deals with a specific two-level optimization for a specific multi-energy system, the methodology and configuration in this work could be applied to other systems. Given GA often involves many iterations, the computational efficiency of the optimisation method could be further explored by investing alternative solving algorithm such as evolutionary program.

6. Acknowledgments

The research is supported by in part by EPSRC through the National Centre for Energy Systems Integration (grant number EP/P001173/1), National Natural Science Foundation of China under Grant No.51806137 and Shanghai Rising-Star Program under grant No. 20QA1404700.

References

[1] A. Ioannou, A. Angus, and F. Brennan, Stochastic Prediction of Offshore Wind Farm LCOE through an Integrated Cost Model, Energy Procedia, vol. 107, no. September 2016, pp. 383–389, 2017.

[2] J. de la Hoz *et al.*, Regulatory-framework-embedded energy management system for microgrids: The case study of the Spanish self-consumption scheme, Appl. Energy, vol. 251, p. 113374, 2019.

[3] P. E. Santangelo and P. Tartarini, Fuel cell systems and traditional technologies. Part I: Experimental CHP approach, Appl. Therm. Eng., vol. 27, no. 8–9, pp. 1278–1284, 2007.

[4] O. Grillo, Hybrid systems for distributed power generation based on pressurisation and heat recovering of an existing 100 kW molten carbonate fuel cell, J. Power Sources, vol. 115, no. 2, pp. 252–267, 2003.

[5] Organisations supporting IEA Bioenergy Task 37 – Energy from Biogas, *The Biogas Handbook*. Elsevier, pp. xxix–xxx, 2013.

[6] E. I. Al-musleh, D. S. Mallapragada, and R. Agrawal, Continuous power supply from a baseload renewable power plant, Appl. Energy, vol. 122, pp. 83–93, 2014.

[7] M. Hosseini, I. Dincer, and M. A. Rosen, Hybrid solar–fuel cell combined heat and power systems for residential applications: Energy and exergy analyses, J. Power Sources, vol. 221, pp. 372–380, 2013.

[8] C. Wang and M. H. Nehrir, Power management of a stand-alone wind/photovoltaic/fuel cell energy system, IEEE Trans. Energy Convers., vol. 23, no. 3, pp. 957–967, 2008.

[9] S. B. Silva, M. Oliveira, and M. M. Severino, "Sizing and Optimization of Hybrid Photovoltaic, Fuel Cell and Battery System," Latin America Transactions, IEEE (Revista IEEE Am. Lat., vol. 9, no. 1, 2011.

[10] H. Yang, W. Zhou, L. Lu, and Z. Fang, Optimal sizing method for stand-alone hybrid solar–wind system with LPSP technology by using genetic algorithm, Sol. Energy, vol. 82, no. 4, pp. 354–367,

2008.

[11] A. Ghaffari and A. Askarzadeh, Design optimization of a hybrid system subject to reliability level and renewable energy penetration, Energy, vol. 193, p. 116754, 2020.

[12] R. Suciu, L. Girardin, and F. Maréchal, Energy integration of CO2 networks and power to gas for emerging energy autonomous cities in Europe, Energy, vol. 157, pp. 830–842, 2018.

[13] J. Gorre, F. Ruoss, H. Karjunen, J. Schaffert, and T. Tynjälä, Cost benefits of optimizing hydrogen storage and methanation capacities for Power-to-Gas plants in dynamic operation, Appl. Energy, vol. 257, no. August 2019, 2020.

[14] P. Colombo, A. Saeedmanesh, M. Santarelli, and J. Brouwer, Dynamic dispatch of solid oxide electrolysis system for high renewable energy penetration in a microgrid, Energy Convers. Manag., vol. 204, p. 112322, 2020.

[15] V. S. Tabar and V. Abbasi, Energy management in microgrid with considering high penetration of renewable resources and surplus power generation problem, Energy, vol. 189, p. 116264, 2019.

[16] T. Choudhary, M. Sahu, and S. KRISHNA, Thermodynamic Analysis of Solid Oxide Fuel Cell Gas Turbine Hybrid System for Aircraft Power Generation, 2017.

[17] T. Choudhary and Sanjay, Thermodynamic assessment of advanced SOFC-blade cooled gas turbine hybrid cycle, Int. J. Hydrogen Energy, vol. 42, no. 15, pp. 10248–10263, 2017.

[18] T. Choudhary and Sanjay, Thermodynamic assessment of SOFC-ICGT hybrid cycle: Energy analysis and entropy generation minimization, Energy, vol. 134, pp. 1013–1028, 2017.

[19] T. Choudhary, M. K. Sahu, S. R, A. Kumari, and A. Mohapatra, Thermodynamic Modeling of Blade Cooled Turboprop Engine Integrated to Solid Oxide Fuel Cell: A Concept. SAE International , 2018.

[20] Y. Cao and T. parikhani, A solar-driven lumped SOFC/SOEC system for electricity and hydrogen production: 3E analyses and a comparison of different multi-objective optimization algorithms, J.

Clean. Prod., vol. 271, p. 122457, 2020.

[21] E. Gholamian, P. Hanafizadeh, A. Habibollahzade, and P. Ahmadi, Evolutionary based multi-criteria optimization of an integrated energy system with SOFC, gas turbine, and hydrogen production via electrolysis, Int. J. Hydrogen Energy, vol. 43, no. 33, pp. 16201–16214, 2018.

[22] Z. Zhang, J. Zhou, Z. Zong, Q. Chen, P. Zhang, and K. Wu, Development and modelling of a novel electricity-hydrogen energy system based on reversible solid oxide cells and power to gas technology, Int. J. Hydrogen Energy, vol. 44, no. 52, pp. 28305–28315, 2019.

[23] X. Ding, X. Lv, and Y. Weng, Coupling effect of operating parameters on performance of a biogas-fueled solid oxide fuel cell/gas turbine hybrid system, Appl. Energy, vol. 254, no. August, p. 113675, 2019.

[24] X. Lv, X. Liu, C. Gu, and Y. Weng, Determination of safe operation zone for an intermediate-temperature solid oxide fuel cell and gas turbine hybrid system, Energy, vol. 99, pp. 91–102, 2016.

[25] L. Zhang, J. Kuang, B. Sun, F. Li, and C. Zhang, A two-stage operation optimization method of integrated energy systems with demand response and energy storage, Energy, vol. 208, p. 118423, 2020.

[26] X. Ding, X. Lv, and Y. Weng, Fuel-Adaptability Analysis of Intermediate-Temperature-SOFC/Gas Turbine Hybrid System With Biomass Gas, J. Energy Resour. Technol., vol. 143, no. 2, Aug. 2020.

[27] W. Sun and G. P. Harrison, Wind-solar complementarity and effective use of distribution network capacity, Appl. Energy, vol. 247, no. June 2018, pp. 89–101, 2019.

[28] C. Gu, C. Tang, Y. Xiang, and D. Xie, Power-to-gas management using robust optimisation in integrated energy systems, Appl. Energy, vol. 236, no. September 2018, pp. 681–689, 2019.

[29] M. Thema, F. Bauer, and M. Sterner, Power-to-Gas: Electrolysis and methanation status review, Renew. Sustain. Energy Rev., vol. 112, pp. 775–787, 2019.

[30] P. Aguiar, C. S. Adjiman, and N. P. Brandon, Anode-supported intermediate temperature direct internal reforming solid oxide fuel cell. I: Model-based steady-state performance, J. Power Sources, vol. 138, no. 1–2, pp. 120–136, 2004.

[31] X. Wang, X. Lv, and Y. Weng, Performance analysis of a biogas-fueled SOFC/GT hybrid system integrated with anode-combustor exhaust gas recirculation loops, Energy, vol. 197, p. 117213, 2020.

[32] H. YAKABE and T. SAKURAI, 3D simulation on the current path in planar SOFCs, Solid State Ionics, vol. 174, no. 1–4, pp. 295–302, 2004.

[33] A. Lazzaretto and A. Toffolo, Energy, economy and environment as objectives in multi-criterion optimization of thermal systems design, Energy, vol. 29, no. 8, pp. 1139–1157, 2004.

[34] F. Zhao and A. V Virkar, Dependence of polarization in anode-supported solid oxide fuel cells on various cell parameters, J. Power Sources, vol. 141, no. 1, pp. 79–95, 2005.

[35] H. I. H. Saravanamuttoo, G. F. C. Rogers, and H. Cohen, No Title, Gas Turbine Theory, 2001.

[36] S. H. Chan, H. K. Ho, and Y. Tian, Modelling for part-load operation of solid oxide fuel cell–gas turbine hybrid power plant, J. Power Sources, vol. 114, no. 2, pp. 213–227, 2003.

[37] X. Lv, X. Ding, and Y. Weng, Catalytic combustion of ultra-low heating value fuels over 0.5%Pd/ZrO2/γ-Al2O3 Catalyst, in *American Society of Mechanical Engineers, Power Division (Publication) POWER*, 2017, vol. 1.

[38] A. Liu and Y. Weng, Performance analysis of a pressurized molten carbonate fuel cell/micro-gas turbine hybrid system, J. Power Sources, vol. 195, no. 1, pp. 204–213, 2010.

[39] W. Short, D. Packey, and T. Holt, A manual for the economic evaluation of energy efficiency and renewable energy technologies, Renew. Energy, vol. 95, no. March, pp. 73–81, 1995.

[40] J. Aldersey-Williams, I. D. Broadbent, and P. A. Strachan, Better estimates of LCOE from audited accounts – A new methodology with examples from United Kingdom offshore wind and CCGT,

Energy Policy, vol. 128, no. December 2018, pp. 25–35, 2019.

[41] V. Eveloy, P. Rodgers, and A. Al Alili, Multi-objective optimization of a pressurized solid oxide fuel cell – gas turbine hybrid system integrated with seawater reverse osmosis, Energy, vol. 123, pp. 594–614, 2017.

[42] Department of Business Energy and Industrial Strategy, BEIS Electricity Generation Costs, no. November, p. 85, 2016.

[43] G. Parks, R. Boyd, J. Cornish, and R. Remick, Hydrogen Station Compression, Storage, and Dispensing Technical Status and Costs: Systems Integration, Relat. Inf. Indep. Rev. Publ. U.S. Dep. Energy Hydrog. Fuel Cells Progr., no. May, p. Medium: ED; Size: 74 pp., 2014.

[44] B. Najafi, A. Shirazi, M. Aminyavari, F. Rinaldi, and R. A. Taylor, Exergetic, economic and environmental analyses and multi-objective optimization of an SOFC-gas turbine hybrid cycle coupled with an MSF desalination system, Desalination, vol. 334, no. 1, pp. 46–59, 2014.

[45] Y. D. Lee, K. Y. Ahn, T. Morosuk, and G. Tsatsaronis, Exergetic and exergoeconomic evaluation of a solid-oxide fuel-cell-based combined heat and power generation system, Energy Convers. Manag., vol. 85, pp. 154–164, 2014.

[46] L. Khani, S. M. S. Mahmoudi, A. Chitsaz, and M. A. Rosen, Energy and exergoeconomic evaluation of a new power/cooling cogeneration system based on a solid oxide fuel cell, Energy, vol. 94, pp. 64–77, 2016.

[47] F. Calise, M. Dentice d'Accadia, A. Palombo, and L. Vanoli, Simulation and exergy analysis of a hybrid Solid Oxide Fuel Cell (SOFC)–Gas Turbine System, Energy, vol. 31, no. 15, pp. 3278–3299, 2006.

Nomenclatures

P2G	Power-to-gas
$c_{p,\mathrm{m}}$	Specific heat capacity for species m
$n_{\mathrm{H_2,fuel}}$	Mole flow rate
T	Temperature
Δh	Enthalpy change of reaction
η_c	Compressor isentropic efficiency
η_t	Turbine isentropic efficiency
η_{hybrid}	Electrical efficiency of system
SOFC	Solid oxide fuel cell
GT	Gas turbine
TIT	Turbine inlet temperature
E^{OCP}	Open circuit potential
M_{fuel}	Molar flowing rate of fuel
P_{SOFC}, P_{GT}	Output power
$P_{\mathrm{C,water}}$, $P_{\mathrm{C,fuel}}$	Power consumed
R	Gas constant
U	Potential
T_{std}	Standard temperature
T_{out}	Outlet temperature
$\varepsilon_{\mathrm{comb}}$	Entropy efficiency of catalytic combustor
H_{cc}	Combustor entrance enthalpy
$Q_{\mathrm{H_2}}$	Enthalpy of combustion
$y^0_{\mathrm{CH_2}}$	Molar fraction of hydrogen
$LHV^0_{\mathrm{H_2}}$, $HHV^0_{\mathrm{H_2}}$	Calorific values of hydrogen
P_{t}	Wind plant power
LCC	Life-cycle cost
REP	Wind curtailment rate